August 27-31, 2023
FLORENCE - ITALY
ICWE 16
16th International Conference on Wind Engineering

Aerodynamic Forces on Domed Free Roofs

Wei Ding [1], Lizhi Wen [2], Yasushi Uematsu [3]

[1] *National Institute of Technology (KOSEN), Akita College, Akita, Japna, tei85@akita-nct.ac.jp*
[2] *Disaster Prevention Research Institute, Kyoto University, Kyoto, Japan, wen.lizhi.87n@st.kyoto-u.ac.jp*
[3] *National Institute of Technology (KOSEN), Akita College, Akita, Japan, uematsu@akita-nct.ac.jp*

SUMMARY:
This paper investigates the characteristics of wind pressures and wind forces on domed free roofs based on a wind tunnel experiment and a CFD analysis using LES. The rise-to-span ratio, *f/D*, was varied from 0.1 to 0.4. The wind tunnel models of 2 mm thickness were made by using a 3D printer. The distributions of wind pressure coefficients along a centerline on both the top and bottom surfaces were measured. The wind pressure distribution on the whole roof was obtained by rotating the model. The results indicate that the contour lines of mean wind pressure coefficients, $\bar{C}_{p,t}$ and $\bar{C}_{p,b}$, on the top and bottom surfaces and the resultant wind force coefficient, $\bar{C}_f$, are almost perpendicular to the wind direction. An empirical formula was provided for the distribution of mean wind force coefficient, $\bar{C}_f$, along the centreline parallel to the wind direction. The distributions of the maximum and minimum peak wind force coefficients, $\hat{C}_f$ and $\check{C}_f$, on the whole roof were also obtained. The results obtained in this paper may provide a useful guidance for structural engineers when estimating the design wind force coefficients.

Keywords: Domed free roof, wind tunnel experiment, CFD, wind pressure distribution, net wind force

1. INSTRUCTION

Free-standing canopy roofs (free roofs) are widely used for buildings providing shade and weather protection in public spaces. Since the roofs are usually supported by only columns, wind action is directly exerted both on the top and bottom surfaces of the roof. As a result, the wind forces on free roofs are rather complicated compared with those on enclosed buildings. Furthermore, free roofs are generally susceptible to dynamic wind actions, because they are generally light-weighted and flexible. Therefore, the wind resistance is one of the major concerns of structural engineers, when designing these structures.

Regarding planar free roofs, such as gable, troughed and mono-sloped roofs, extensive researches have been conducted by several researchers, and the wind force coefficients for these roofs are specified in codes and standards, e.g., (ASCE 7, 2017) and (AIJ, 2015) and so on. By comparison, only a few studies have been performed on the wind loading of curved free roofs. For example, (Natalini et al. 2013) investigated the wind forces on vaulted free roofs in a wind tunnel. They measured only the mean wind pressures acting on the roof. No discussion was made of the dynamic load effect of turbulent winds. (Pagnini et al. 2022) measured the distributions of mean and peak wind force coefficients on a vaulted free roof. (Uematsu and Yamamura, 2019) investigated the wind force coefficients for designing the main wind force resisting systems of

vaulted free roofs based on the results of the overall aerodynamic forces and moments measured by a six-component force balance. Hyperbolic paraboloid (HP) is often used for free roofs composed of membranes. Wind loads on HP-shaped free roofs were studied experimentally by (Uematsu et al. 2014), in which the dynamic load effects of turbulent winds were considered. However, as for domed free roofs, only (Uematsu and Yamamura, 2019) made an experimental study of wind loads on such roofs, to the authors' best knowledge.

The purpose of this study is to investigate the characteristics of the wind pressures on domed free roofs based on a wind tunnel experiment and a CFD analysis using LES. Only the wind tunnel experiment is described here due to space limitation. The results may provide an important reference for structural engineers when discussing the design wind loads on domed free roofs.

2. WIND TUNNEL EXPERIMENT

2.1. Wind Tunnel Flow and Model

The experiment is carried out in a turbulent boundary layer; the power-law exponent α for the mean wind speed profile is approximately 0.27; and the intensity I_u and the integral scale L_x of turbulence at a height of z = 10 cm are approximately 0.2 and 0.2 m, respectively. Regarding the details of the wind tunnel flow, see (Ding and Uematsu, 2022).

Fig. 1a shows a wind tunnel model with a rise-to-span ratio (f/D) of 0.3. The models used in this study are the same as those used in (Uematsu and Yamamura, 2019). The models are made by using a 3D printer. The notation and the coordinate system used in this paper are illustrated in Fig. 1b. The geometric scale λ_L is assumed 1/100. The span D and the mean roof height H are fixed to 150 mm and 80 mm, respectively. The rise-to-span ratio f/D ranges from 0.1 to 0.4. Therefore, the heights of roof top and eaves depend on f/D. The roof is supported by four columns of 6.5 mm outside diameter. The roof thickness is 2 mm. Nine pressure taps of 0.6 mm inside diameter are installed along a centerline both on the top and bottom surfaces, as shown in Fig. 1c, to obtain the net wind forces acting on the roof. The wind direction θ is changed from 0° to 90° at an increment of 5°, providing the net wind force distribution over the whole roof.

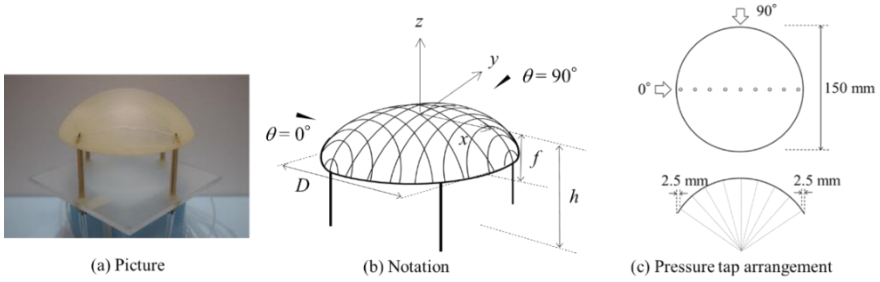

Figure 1. Experimental model

2.2. Experimental Procedure

The wind speed U_H at the mean roof height H is set to 9 m/s. The velocity scale λ_V is assumed 1/2.4, resulting in the time scale of λ_T (= λ_L/λ_V) = 1/42. The pressure taps are connected to a multi-channel pressure transducer via flexible vinyl tubes of 1 mm inside diameter. The total length of tubing is 1 m. Wind pressures at all pressure taps are sampled simultaneously at a rate of 500 Hz for a time duration of 14.3 s, which is equivalent to 10 min at full scale. A low-pass filter with a cut-off frequency of 300 Hz is used to remove high-frequency noise from the signals. The distortion of the measured pressures due to the tubing system is compensated by the transfer function of the measuring system in the frequency domain. The measurements are repeated 10

times under each experimental condition. The wind pressure P is converted to a pressure coefficient $C_p(=(P-P_s)/q_H)$, where P_s represents the static pressure and q_H $(=\frac{1}{2}\rho U_H^2$, with ρ being the air density) represents the dynamic pressure of the approach flow at the mean roof height H. The wind pressure coefficients on the top and bottom surfaces of the model are represented by $C_{p,t}$ and $C_{p,b}$, respectively. The net wind force per unit area acting on the roof is given by the difference between the pressures on the top and bottom surfaces, which is normalized by q_H. As a result, the wind force coefficient C_f is represented by $C_{p,t}-C_{p,b}$.

3. CHARACTERISTICS OF WIND PRESSURES AND WIND FORCES ACTING ON THE ROOF

3.1. Mean wind pressure and wind force coefficients

Fig. 2 shows the distributions of the mean wind pressure coefficients, $\bar{C}_{p,t}$ and $\bar{C}_{p,b}$, on the top and bottom surfaces of the roof and the mean wind force coefficients, $\bar{C}_f$, when *f/D* = 0.2, in which the distributions are illustrated by contour lines. It is found that the contour lines are roughly perpendicular to the wind direction. Similar results were obtained for the other models with *f/D* = 0.1, 0.3 and 0.4. Then, the main focus is on the distributions along the centerline parallel to the wind direction. Fig. 3 shows the distributions of mean wind force coefficients $\bar{C}_f$ along the centerline. The $\bar{C}_f$ distribution can be approximated by the Eq. (1).

$$\bar{C}_f = \sum_{i=0}^{4} a_i \cos\frac{i\pi s}{s_{\max}} \tag{1}$$

where the coefficients a_i are determined by using the least square method, as shown in Table 1. The empirical formula is compared with the experimental results in Fig. 3. The results can be used for estimating the wind loads for the main wind force resisting systems of domed free roofs.

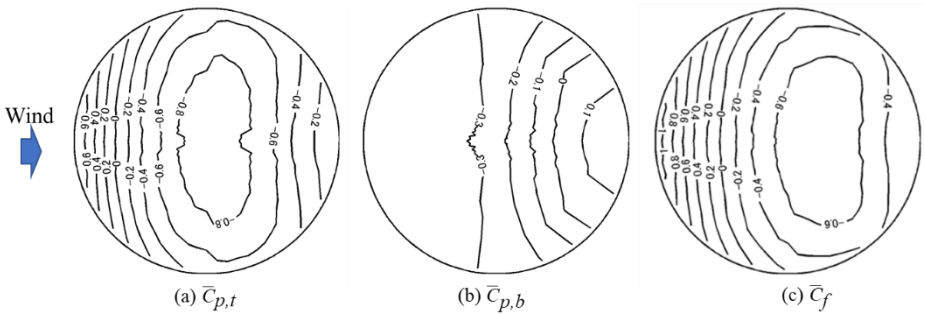

Figure 2. Distributions of mean wind pressure and wind force coefficients on the roof (*f/D* = 0.2)

3.2. Maximum and minimum peak wind force coefficients

Roof cladding and components are generally designed based on the positive and negative peak wind force coefficients. In this paper, we focus on the ensemble averages of the maximum and minimum peak wind force coefficients, $\hat{C}_f$ and $\check{C}_f$, obtained from the ten-time measurements in the wind tunnel experiment. Fig. 4 shows the distributions of $\hat{C}_f$ and $\check{C}_f$ over the whole roof when *f/D* = 0.2. Similar results were obtained for the other *f/D* ratios. It is found that very large $\hat{C}_f$ values occur in the windward area, which are due to a combination of large $C_{p,t}$ values (positive) and large magnitude $|C_{p,b}|$ values (negative). On the other hand, the magnitude of $\check{C}_f$

becomes large in the top area. This is due to large peak suctions on the top surface in this area. Because the values of $C_{p,b}$ in this area are negative, the magnitude of $\check{C}_f$ is smaller than that of $\hat{C}_f$ in the windward area.

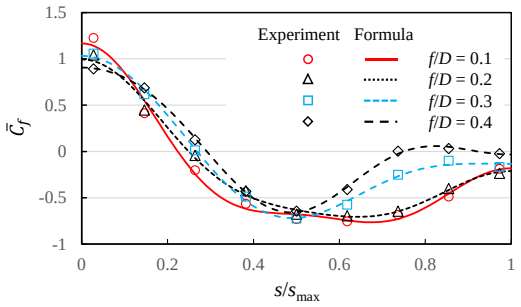

Figure 3. Distributions of mean wind force coefficients along the centreline parallel to the wind direction (experiment and formula)

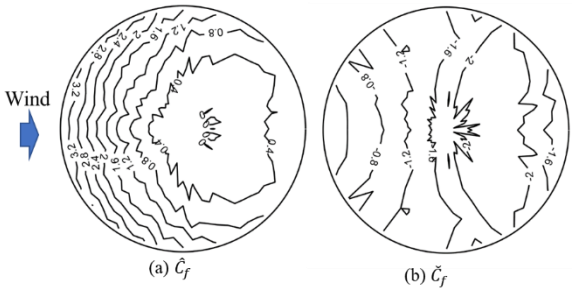

Figure 4. Distributions of the maximum and minimum peak wind force coefficients (*f*/*D* = 0.2)

Table 1. The values of coefficients a_i in the empirical formula, Eq. (1)

	f/*D* = 0.1	*f*/*D* = 0.2	*f*/*D* = 0.3	*f*/*D* = 0.4
a_0	–0.265	–0.218	–0.101	0
a_1	0.530	0.522	0.415	0.312
a_2	0.586	0.511	0.584	0.545
a_3	0.144	0.081	0.167	0.158
a_4	0.172	0.098	–0.033	–0.109

4. CONCLUSIONS

The characteristics of wind pressures on domed free roofs were investigated based on a wind tunnel experiment and a CFD analysis using LES. The contour lines of mean wind pressure and force coefficients were almost perpendicular to the wind direction. An empirical formula was provided for the distribution of the mean wind force coefficients along the centerline parallel to the wind direction. Furthermore, the distributions of the maximum and minimum peak wind force coefficients were presented.

ACKNOWLEDGEMENTS

This research is financially supported by the Nomura Membrane Technology Promotion Foundation (2018).

REFERENCES

American Society of Civil Engineers, 2017. Minimum Design Loads and Associated Criteria for Buildings and Other Structures. ASCE/SEI 7-16, Reston, VA.

Architectural Institute of Japan, 2015. Recommendations for Loads on Buildings (2015).

Ding, W., Uematsu, Y., 2022. Discussion of design wind loads on a vaulted free roof. Wind, 2, 479-494.

Natalini M.B., Morel C., Natalini B., 2013. Mean loads on vaulted canopy roofs. Journal of Wind Engineering and Industrial Aerodynamics, 119, 102–113.

Pagnini, L., Torre, S., Freda, A., Piccardo, G., 2022. Wind pressure measurements on a vaulted canopy roof, Journal of Wind Engineering and Industrial Aerodynamics. 223, 104934.

Uematsu Y., Miyamoto Y., Gavanski E., 2014. Wind loading on a hyperbolic paraboloid free roof. Journal of Civil Engineering and Architecture, 8(10), 1–19.

Uematsu, Y., Yamamura, R., 2019. Wind loads for designing the main wind-force resisting systems of cylindrical free-standing canopy roofs. Technical Transactions, Civil Engineering, 7, 124-144.

Uematsu, Y., Yamamura, R., 2019. Experimental study of wind loads on domed free roofs. Proceedings of the XV Conference of the Italian Association for Wind Engineering, IN-NENO 2018, Lecture Note in C.E., 27, 716-729.